J. Indian Chem. Soc.,
Vol. 97, January 2020, pp. 11-19

Investigation of swelling and antibacterial properties of carboxymethyl chitosan/poly(vinyl alcohol) nanocomposite hydrogel beads containing ZnO nanoparticles

Iman Gholamali[a], Manzarbanou Asnaashariisfahani*[a], Eskandar Alipour[a] and Abbas Akhavan Sepahi[b]

[a]Department of Chemistry, North Tehran Branch, Islamic Azad University, P.O. Box 19585/936, Tehran, Iran

E-mail: m_asnaashari@iau-tnb.ac.ir

[b]Department of Microbiology, Faculty of Science, North Branch, Islamic Azad University, Tehran, Iran

Manuscript received online 21 October 2018, revised 23 December 2019, accepted 24 December 2019

The CsMe/PVA/ZnO nanocomposite hydrogel beads have been introduced a new technique, which is dependent on pH. They were prepared successfully *in situ* by forming of ZnO nanoparticles within swollen CsMe/PVA hydrogel beads. The resulting hydrogel beads were examined by running various experimental procedures such as FT-IR, XRD, EDX and SEM. XRD and EDX patterns verified the formation of ZnO nanoparticles in the bead networks; moreover, the formation of ZnO nanoparticles with size range from 44 to 88 nm within the bead matrix was confirmed by SEM micrographs. The prepared nanocomposite hydrogel beads showed a pH-sensitive swelling behavior. The results showed that the prepared nanocomposite hydrogel beads outperformed the pure CsMe/PVA hydrogel beads in terms of swelling capacity in various pH values and salt solutions. The antibacterial activity of the nanocomposite hydrogel beads was examined and mechanisms involved in their synthesis were reported; the results showed an excellent antibacterial behavior of the nanocomposite hydrogel bead.

Keywords: Carboxymethyl chitosan, poly(vinyl alcohol), hydrogel, nanocomposite, zinc oxide nanoparticles.

Introduction

Hydrogels are a class of materials with the three-dimensional network of a polymer that can absorb a high amount of water or biological fluids, without being soluble under physiological conditions[1]. Also, due to their excellent properties, such as high swelling ratio, non-toxicity, biocompatibility and biodegradability hydrogels would have basic roles in agriculture[2,3], and biomedical applications including wound dressing[4], tissue engineering[5,6] and controlled drug and protein delivery[7].

Chitosan is one of the most abundant natural cationic polymers produced commercially by deacetylation of chitin. Due to its unique polycationic nature, it has been widely applied in medical and pharmaceutical fields[9,10]. Chitosan nanocomposite hydrogels revealed a higher swelling and good antibacterial effects against *Escherichia coli* and *Staphylococcus aureus* bacteria[11,12]. Carboxymethyl chitosan (CsMe) is a biodegradable and biocompatible polymer obtained from the reaction of chitosan with monochloroacetic acid and in an alkaline medium[13]. CsMe has several advantages over chitosan such as increased water solubility, increased antioxidant property[14] high moisture retention ability[15] and higher antibacterial activity[9,16] that Wahid *et al*. prepared and characterized antibacterial CsMe/ZnO nanocomposite hydrogels by *in situ* formation of ZnO nanoparticles in CsMe hydrogel matrix. Therefore, carboxymethylation of chitosan is a promising approach in a number of environmental, biomedical, and pharmaceutical applications[17,18].

Poly(vinyl alcohol) (PVA) is a water soluble polymer, which has been studied intensively due to its excellent chemical stability, easy preparation, film-forming ability, biocompatibility, gel forming and physical properties[19–21]. PVA hydrogels are relevant for biomaterial and pharmaceutical applications such as drug delivery, wound dressing, contact lenses, and artificial organs[22,23] that Ahmadian *et al*. studied on synthesis of PVA/CuO nanocomposite hydrogels applicable in a drug delivery system. Agnihotri *et al.* studied the chemical crosslinking of chitosan with a polymer owning to good chemical resistance, greater mechanical strength and hydrophilicity including PVA that may lead to the formation of a hydrogel composite for antibacterial applications[24].

Recently, there has been a great interest to generate antibacterial hydrogels because of their superior biomedical relevance[25]. Among antibacterial hydrogels, inorganic-based nanocomposite hydrogel beads are particularly promising for bacterial inactivation applications in materials and engineering science. These antibacterial agents possess a great potential to inhibit microbial growth. Because of they are easily functionalized with inorganic materials and biocompatible, this characteristic makes them attractive in the biomedical and biotechnological fields[17,18]. Among them, silver based materials are of special interest owing to their broad spectrum inhibitory and strong bactericidal effect[26]. During the last few years, there has been an increased interest in silver nanocomposite hydrogels as an antimicrobial agent in the medical field[27–30]. Nanocomposites are a combination of biopolymers and inorganic materials, mainly metals like silver, copper, TiO_2, and ZnO in nano-dimensions. Superior mechanical strength, high thermal resistance and low permeability against gases and water vapor are a number of the properties of bio-nanocomposites. In recent years, bio-nanocomposites have been used as wound dressings and tissue engineering as well[31–33]. The main advantage using inorganic nanoparticles accompanied with the organic antimicrobial mediators are their strength, stability, and extended shelf life; besides, they can be used potentially for biomedical field[34].

Considering these facts, the objective of this study was to prepare and characterize a group of carboxymethyl chitosan/poly(vinyl alcohol) hydrogel beads containing ZnO nanoparticles. Novel CsMe/PVA/ZnO nanocomposite hydrogel beads were successfully prepared by *in situ* formation of ZnO nanoparticles in the CsMe/PVA hydrogel matrix. The resulting nanocomposite hydrogel beads were characterized using FT-IR, XRD, EDX and SEM analyses. The effect of the concentration of the ZnO nanoparticles on the swelling in different aqueous mediums and antibacterial activity for the Gram-negative *E. coli* and Gram-positive *S. aureus* bacteria was investigated.

Results and discussion

Scheme 1 schematically represents the formation of ZnO nanoparticles in CsMe/PVA hydrogel network. A bond is

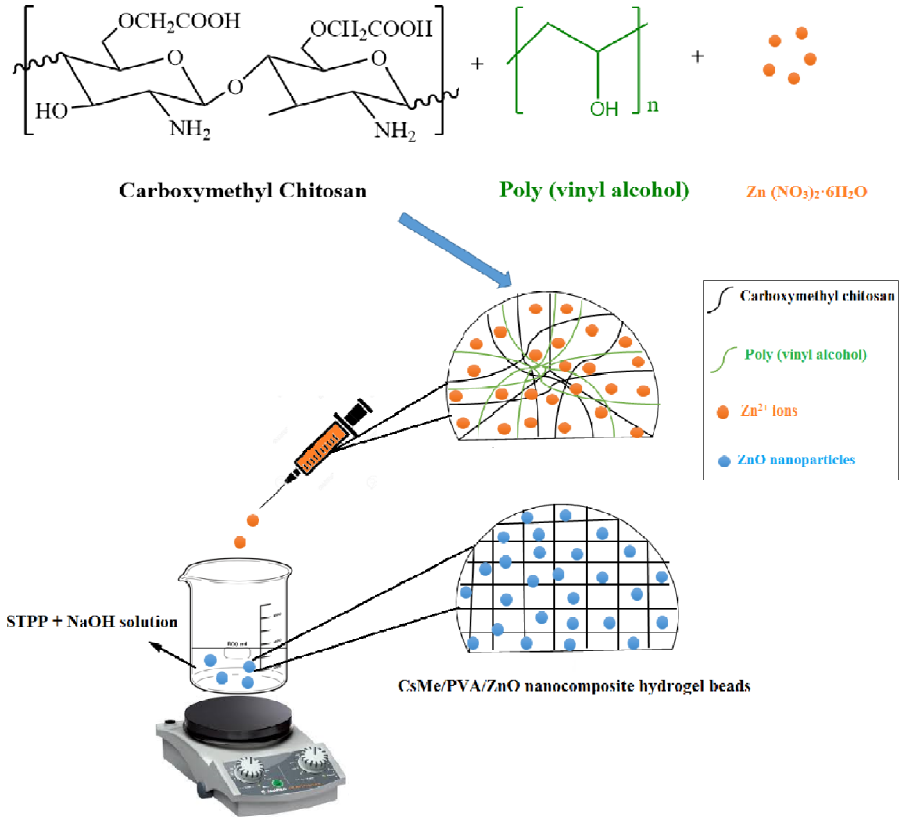

Scheme 1. The schematic representation of *in situ* formation of ZnO nanoparticles in CsME/PVA hydrogel network.

formed between the CsMe/PVA hydrogels and the positively charged Zn^{2+} in aqueous solutions of zinc nitrate by electrostatic interactions due to negatively charged carboxylate and alkolate groups of CsMe/PVA ($-CO_2^-$, $-CH_2O^-$)[16,24]. Zinc ions were converted to ZnO nanoparticles with the suitable basic agent (NaOH solution). The ZnO nanoparticles were prepared *in situ* through a simple and cost-effective process that did not require heating or any other tools for synthesis[1,35].

FT-IR analysis:

Fig. 1a displays the characteristic absorption peaks of the four components; CsMe, PVA and ZnO nanoparticles. The FT-IR spectrum of the CsMe, a broad peak 3407 cm^{-1} is related to the stretching vibrations of -NH and -OH functional groups[36,37]. Also, FT-IR spectrum of CsMe includes several peaks at 1591, 1410 and 1121 cm^{-1} related to C-O stretching and the bending modes of the N-H, C-N stretching and C-OH stretching on the polysaccharide skeleton, respectively[31]. The FT-IR spectrum of the PVA, a broad peak 3345 cm^{-1} is related to hydroxyl groups and several peaks at 2921 cm^{-1} is associated to C-H stretching of CH_2, 1416 cm^{-1} and 1100 cm^{-1} is related to CH_2 scissoring and C-O stretching. FT-IR spectrum of ZnO nanoparticles includes absorption peaks at 440 cm^{-1} associated to Zn-O stretching.

Fig. 1b showed FT-IR spectra of the pure CsMe/PVA hydrogel bead and CsMe/PVA/ZnO nanocomposite hydrogel bead. In Fig. it is showed that the peaks absorption of O-H at 3417 cm^{-1} and 3345 cm^{-1} are attributed to intramolecular hydrogen bond pure hydrogel and nanocomposite hydrogel. Compared with the FT-IR spectra of pure CsMe/PVA hydrogel bead, CsMe/PVA/ZnO nanocomposite hydrogel bead indicated the new peaks in the 400–800 cm^{-1} regions. These peaks were attributed to the incorporation of M-O and O-M-O bonds into the hydrogel.

XRD analysis:

The XRD patterns of the CsMe/PVA/ZnO nanocomposite hydrogel bead and pure CsMe/PVA hydrogel in the 2θ range of 2–70° are shown in Fig. 2. The diffractogram of CsMe/PVA/ZnO nanocomposite hydrogel bead is assigned to diffractions at 2θ values five peaks of 31°, 34°, 36°, 47° and 56° which are attributed to the (100), (002), (101), (102) and (103) crystal planes of ZnO with hexagonal wurtzite structure. All the peaks match well with those of monoclinic phase ZnO crystals and confirm the formation of ZnO particles in the

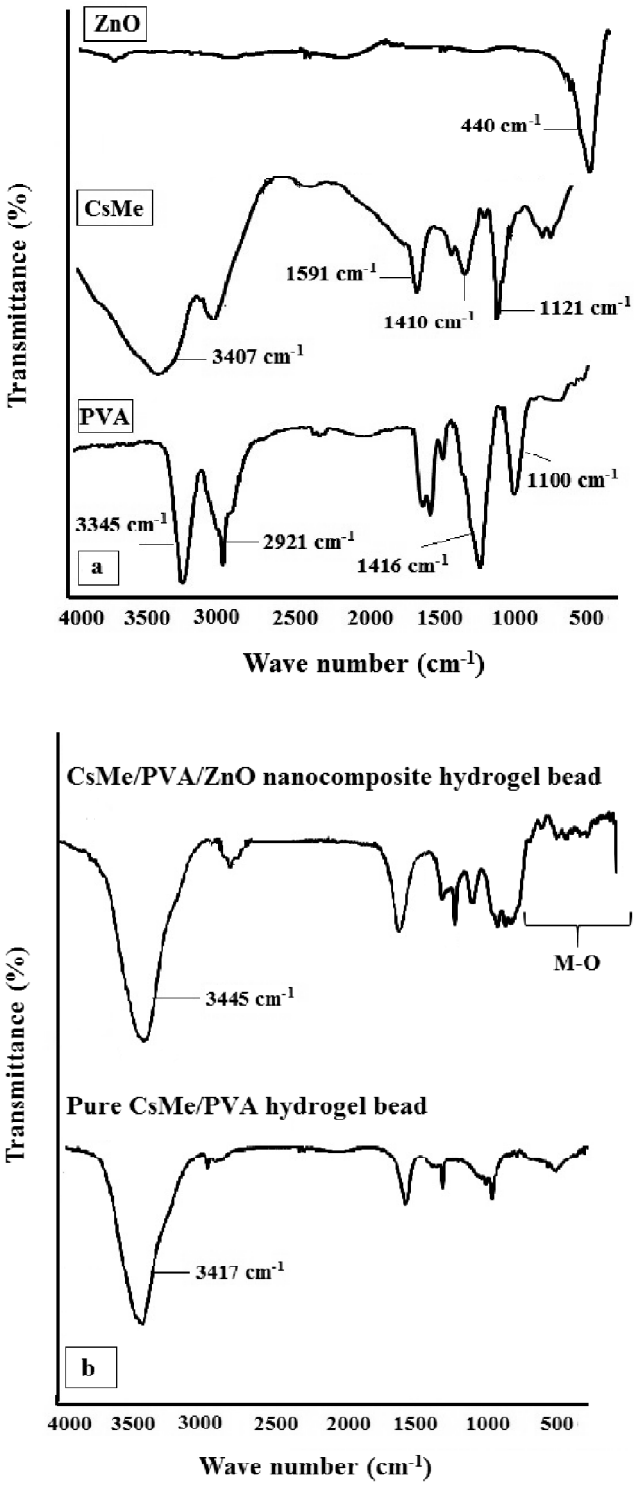

Fig. 1. FT-IR spectra of (a) pure CsMe, PVA and ZnO nanoparticles; (b) pure CsMe/PVA hydrogel bead and CsMe/PVA/ZnO nanocomposite hydrogel bead.

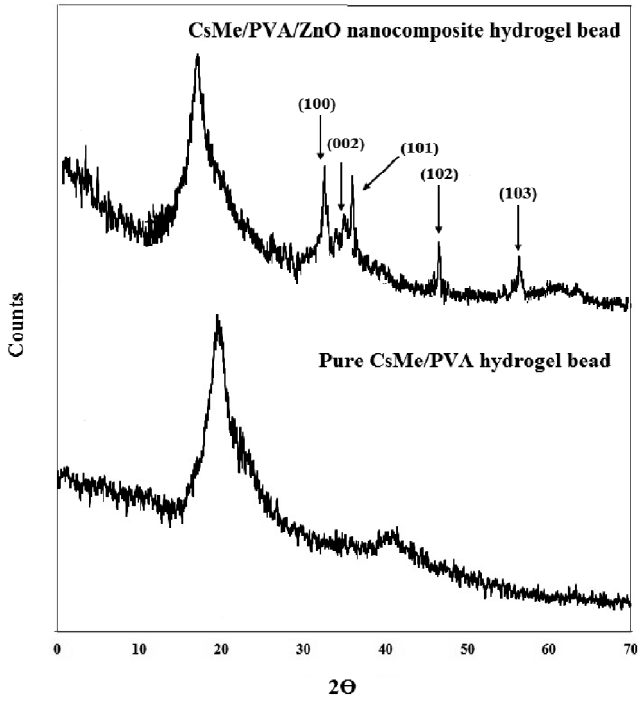

Fig. 2. XRD pattern of pure CsMe/PVA hydrogel bead and CsMe/PVA/ZnO nanocomposite hydrogel bead.

CsMe/PVA hydrogel matrix. None of other peaks can be observed in the XRD pattern that indicate the high purity of obtained ZnO particles[1,39]. A wide peak at 20° is due to the polymer networks.

Scanning electron microscopy (SEM) and energy dispersive X-ray spectroscopy (EDX):

Scanning electron microscopy (SEM) was employed for investigation of the surface morphology of the samples, shape, size and porosity of the hydrogel matrices. SEM of the pure hydrogel bead and CsMe/PVA/ZnO nanocomposite hydrogel beads at ×100,000 magnification are given in Fig. 3. The morphological of surface of the pure CsMe/PVA hydrogel bead indicated numerous wrinkles and several cavities because the hydrogel network collapsed incompletely during drying. The nanocomposite hydrogel beads of CsMe/PVA/ZnO showed a smooth and uniform surface morphology. These results seemed due to interfacial interactions of ZnO nanoparticles with the CsMe/PVA macromolecules that the ZnO nanoparticles could contract and hinder the movability of the CsMe/PVA chains, then changing the surface morphology. After examining the hydrogels, the nanoparticles were observed more clearly on the surface of the nanocomposite hydrogel beads including 0.5% ZnO nanoparticles content with the particle size range was between 44 and 63 nm (Sample Zn1) and some aggregation and bigger particle sizes (51–88 nm) can be seen for the CsMe/PVA/ZnO nanocomposite hydrogel beads containing the highest zinc nitrate concentration of 1.5% (Sample Zn3).

Fig. 4 shows the EDX results of CsMe/PVA/ZnO nanocomposite hydrogel beads. The element information and distribution of elements in hydrogel structure were obtained using EDX analysis that indicates the structure of nanocomposite hydrogel beads contains ZnO nanoparticles. Four typical elements on the CsMe/PVA/ZnO hydrogel beads surface are C, O, N, and Zn shown in Fig. 4[31,38,39].

Antibacterial activity:

The *in vitro* antibacterial properties of CsMe/PVA/ZnO nanocomposite hydrogel beads were tested comparatively against Gram-negative (*E. coli*) and Gram-positive (*S. aureus*) bacteria by disk diffusion test. Inhibition zone under and

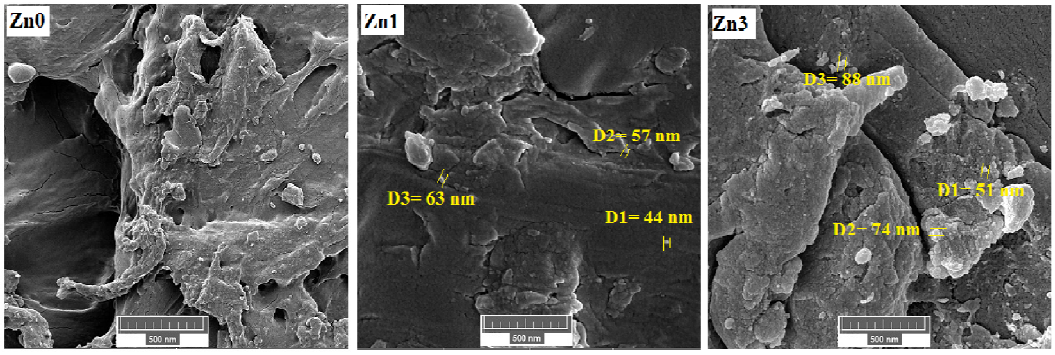

Fig. 3. SEM images of pure CsMe/PVA hydrogel bead (Zn0) and CsMe/PVA/ZnO nanocomposite hydrogel beads with prepared different concentrations of zinc nitrate: 0.5% and 1.5% (Zn1 and Zn3).

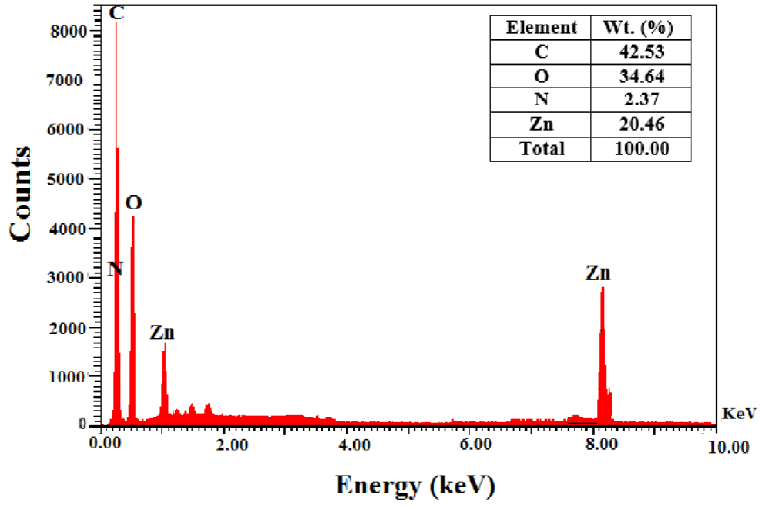

Fig. 4. The EDX of CsMe/PVA/ZnO nanocomposite hydrogel bead.

around the tested samples for bacterial growth was detected visually and listed in Table 1. The inhibition zones are presented in Fig. 5. The results suggest that the ZnO embedded nanocomposite hydrogel beads revealed a more toxic effect on bacteria than pure hydrogel under similar conditions as evidenced by higher inhibition zone. The antibacterial effect of CsMe/PVA/ZnO nanocomposite hydrogel beads could be associated to the attachment of ZnO nanoparticles to the cell wall of bactericides which damages the cell wall and causing leakage of proteins and other intracellular constituents and ultimately causes cell death[40–42]. The results in the Table 1 show that the antibacterial efficiency of the nanocomposite hydrogels is influenced by the concentration of the ZnO nanoparticles regardless of the kind of bacterial used. Hydrogels with more ZnO nanoparticles demonstrate greater antibacterial properties. From the results, we revealed that CsMe/PVA/ZnO nanocomposite hydrogel beads showed better activity towards Gram-negative bacteria than Gram-positive.

Table 1. Antibacterial activity data of CsMe/PVA/ZnO nanocomposite hydrogel beads against *E. coli* and *S. aureus*

Sample code	Inhibition zone (mm)	
	E. coli	*S. aureus*
Zn0	0	0
Zn1	9	5
Zn2	13	8
Zn3	17	12

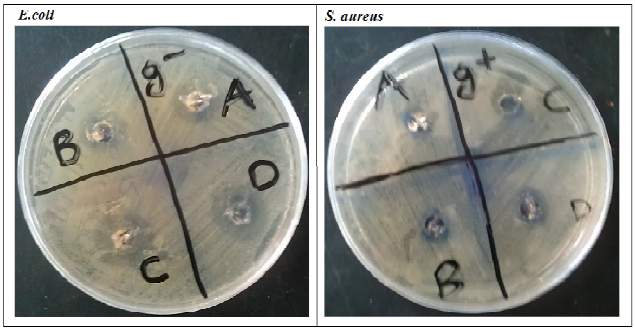

Fig. 5. Antibacterial activity test of CsMe/PVA/ZnO nanocomposite hydrogel beads against *E. coli* and *S. aureus* containing free of ZnONPs (a), 0.5% ZnONPs (b), 1% ZnONPs (c), 1.5% ZnONPs (d).

Effect of pH on swelling behavior:

The swelling behavior of the hydrogel beads was studied in the pH range of 2 to 10 in order to investigate the pH-sensitivity of the prepared hydrogel beads. As shown in the Fig. 6, the swelling of all the hydrogel beads increased with the increase of the pH from 2 to 7, however, it decreased at higher pH values (pH > 7). With increasing pH from 2 to 7, carboxyl and hydroxyl groups on the CsMe and PVA chains converted to negatively charged carboxylate and alkolate ions, resulting in higher electrostatic repulsion and water would be taken up[43,44]. Although we expected to see a rise in the swelling at higher pH values (pH > 7), but a reducing pattern observed at pH > 7, the higher concentration of Na^+ cations shielded the carboxylate and alkolate ions and pre-

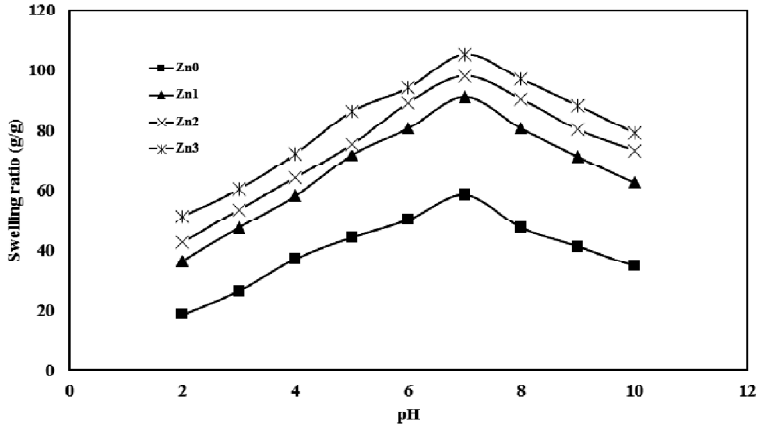

Fig. 6. Swelling behavior of ZnO nanocomposite hydrogel beads at different pH values.

venting complete anion-anion repulsion and restrain the extending of the tangled molecular chain of the hydrogel[45].

In addition, the results in the Fig. 6 show that ZnO nanocomposite hydrogel beads revealed a higher swelling capacity, compared to the neat CsMe/PVA hydrogel. The improvement of the swelling capacity of the ZnO nanocomposite hydrogel beads may be attributed to the presence of ZnO nanoparticles with different size, morphology and surface charges. Charged ZnO nanoparticles results in the penetration of more water molecules to balance the build-up ion osmotic pressure, which causes the hydrogel to swell[46–48]. Furthermore, formation of ZnO nanoparticles in the hydrogel network can expand the hydrogel network and increase the pores and free spaces within the networks and as a consequence adsorbs more water[49,50].

Swelling behavior in saline solutions:

The swelling of the superabsorbent composite depends on the type and valence of the cations. The equilibrium swelling data obtained from the chloride salt solutions of sodium, calcium and aluminum with same concentration are given in Fig. 7. As shown, cation charge has a great influence on swelling capacity. As shown in Fig. 7, multivalent cations decrease the swelling capacity considerably. This dramatic decrease in the water absorbency in multivalent cationic solutions could be due to the complexing ability of the carboxylate groups with multivalent cations. Formation of intramolecular and intermolecular complexes resulted in an increase in the crosslinking density of the network. Therefore, absorbency for the hydrogel in the studied salt solutions is in the order of monovalent > divalent > trivalent cations. Similar

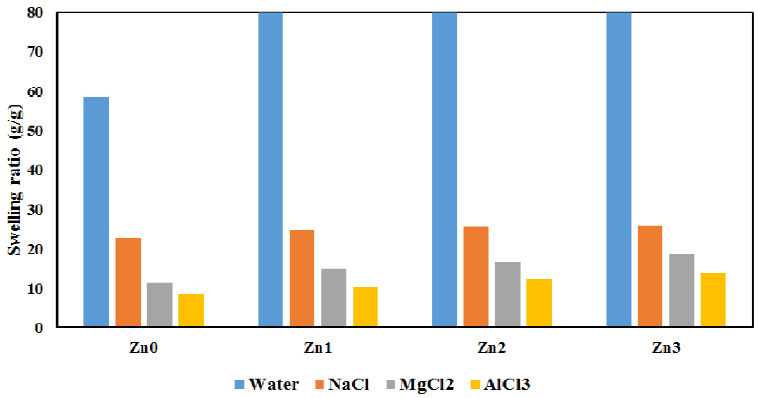

Fig. 7. Swelling behavior of ZnO nanocomposite hydrogel beads in different salt cation solutions (the NaCl, $CaCl_2$ and $AlCl_3$ concentrations were chosen 0.2 *M*).

results have been reported in previous studies[51]. According to this Fig. ZnO nanocomposite hydrogel beads have rather higher absorbencies in salt solutions in comparison with pure hydrogel.

Conclusion

In this project, antibacterial CsMe/PVA/ZnO nanocomposite hydrogel beads were prepared based on the combination of ZnO nanoparticles and biopolymer carboxymethyl chitosan and poly(vinyl alcohol). Pure CsMe/PVA hydrogel bead and CsMe/PVA/ZnO nanocomposite hydrogel beads were successfully synthesized via crosslinking with STPP in an alkaline medium. Structural details of CsMe/PVA/ZnO nanocomposite hydrogel beads were provided by FT-IR, XRD, EDX and SEM analysis. In addition, their swelling behavior was studied at various pH values and salt solutions. XRD and EDX analysis studies confirmed the formation of ZnO nanoparticles in the hydrogel matrix. SEM micrographs clearly showed that ZnO nanoparticles with size ranging from 44–88 nm were formed within the hydrogel matrix, and the number of ZnO nanoparticles increased with the increase of Zn^{2+} concentration. The swelling capacity of the ZnO nanocomposite hydrogel beads was dependent on the abundance of the zinc oxide nanoparticles in the CsMe/PVA hydrogel beads. The swelling of the nanocomposite beads increased with increasing the zinc nitrate concentration and is found to be pH dependent. Swelling capacity for these hydrogel beads in salt solutions with the same concentration is in order of NaCl > $CaCl_2$ > $AlCl_3$. Antibacterial activity of the prepared nanocomposite hydrogel beads was studied against *E. coli* (Gram-negative) and *S. aureus* (Gram-positive) using the agar diffusion test. The results showed an excellent antibacterial activity for CsMe/PVA/ZnO nanocomposite hydrogel beads. CsMe/PVA has several advantages over Cs/PVA such as higher swelling and antibacterial activity that other authors have been reported.

Experimental

Materials:

Chitosan (medium molecular weight and viscosity 200–800 cp), poly(vinyl alcohol) (PVA, molecular mass of 72000), monochloroacetic acid (99%), sodium tripolyphosphate (STPP, technical grade 85%), $Zn(NO_3)_2.6H_2O$, NaOH and methanol were purchased from Merck Co. and used as received.

Methods:

Preparation of carboxymethyl chitosan:

Carboxymethyl chitosan (CsMe) was prepared using the following procedure: 5 g of chitosan was dissolved in 20% w/v NaOH solution for 15 min. 15 g of monochloroacetic acid was then added dropwise to the mixture with constant mechanical stirring for 2 h at T = 40°C until a homogenous mixture was obtained. The obtained mixture was neutralized with 10% acetic acid, poured into an excess of 70% methanol, filtered using a G2 sintered glass funnel, and washed several times with methanol to remove the residual NaOH and monochloroacetic acid. Finally, the obtained CsMe powder was dried in a vacuum oven at T = 55°C for 8 h.

Preparation of crosslinked CsMe/PVA/ZnO nanocomposite hydrogel beads:

CsMe powder was first dissolved in 100 ml distilled water containing 3 wt% NaOH at ambient temperature with constant stirring overnight until a clear homogeneous solution was obtained. PVA solution was dissolved in distilled water with continuous stirring at T = 95°C for 2 h. After cooling at ambient temperature, the CsMe solution was combined with PVA solution by stirring for 2 h in order to obtain a homogenous solution of the two polymers. Sodium tripolyphosphate (STPP) and NaOH were used as the crosslinking agent and oxidizing agent. The desired amount of $Zn(NO_3)_2.6H_2O$ (0%, 0.5%, 1.0% and 1.5%) were added to the mixture solution and stirred until a clear homogeneous viscose solution obtained. Thereafter, the solution was extruded in the form of droplets, using a syringe (2 mm diameter), into an aqueous solution (400 ml) containing STPP (4 g) and NaOH (3.2 g). The beads were stayed in the solution for 24 h in order to crosslink with STPP and also converting Zn^{2+} ions into ZnONPs. After the oxidation of the bound ZnO ions, the beads were washed with distilled water and finally dried under vacuum for 24 h. The CsMe/PVA/ZnO nanocomposite hydrogel beads with 0%, 0.5%, 1.0% and 1.5% of $Zn(NO_3)_2.6H_2O$ content will be referred to as Zn0, Zn1, Zn2 and Zn3 respectively in following lines.

Characterization and analysis:

Infrared spectra was recorded on a FT-IR spectrometer (Bruker Instruments, model Aquinox 55, Germany) in the wave number ranging 4000–400 cm^{-1} at a resolution of 0.5 cm^{-1} as KBr pellets. The X-ray diffraction pattern of the samples were verified with Siemens-D500 diffractometer

using Cu-kα radiation at 35 kV in the scan range of 2θ from 2 to 70° and scan rate of 1°/min. All of analyzed samples were in powdery form. The morphology of the dried neat hydrogel and nanocomposite hydrogels was examined by scanning electron microscope (SEM) (TESCAN MIRA) after coating the dried hydrogels with gold and silver films.

Antibacterial activity:

Antibacterial experiments were studied against both *S. aureus* (Gram-positive) and *E. coli* (Gram-negative) bacteria by agar diffusion test. For agar diffusion method, samples exposed to bacteria in solid media (nutrient agar), and the inhibition zone around samples was determined as the antibacterial effect of ZnO nanoparticles. The agar plates were inoculated with 100 μL spore suspensions of bacteria. The swelled hydrogels, each of which contained test materials at the same size were cut and placed on the agar plate, then incubated with bacterial suspension at 37°C for 24 h.

Swelling behavior:

Swelling ratio of CsMe/PVA/ZnO nanocomposite hydrogel beads were measured according to the previously reported methods[33]. 0.1 g of powdered CsMe/PVA/ZnO nanocomposite hydrogel beads were immersed in 50 ml of aqueous solutions with desired pH at room temperature for 24 h to reach maximum swelling equilibrium. The swelling ratio of nanocomposite hydrogel beads was determined according to eq. (1).

$$\text{Swelling ratio (SR\%)} = W_2 - W_1/W_1 \times 100 \quad (1)$$

where W_1 is initial weight of sample, and W_2 is the weight of the sample after swelling for 24 h. To prepare the pH media, standard HCl (1.0 *M*) and NaOH (1.0 *M*) solutions were diluted with distilled water to reach the desired acidic and basic pHs, respectively.

The water absorbency of the hydrogels in aqueous solutions of the salts (0.2 *M* of NaCl, $CaCl_2$, and $AlCl_3$) was determined in a similar manner.

References

1. I. Gholamali, S. N. Hosseini, E. Alipour and M. Yadollahi, *Starch/Stärke.,* 2019, **71(3-4)**.
2. F. Ullah, M. B. H. Othman, F. Javed, Z. Ahmad and H. M. Akil, *Mater. Sci. Eng. C*, 2015, **57**, 414.
3. T. Wu, Y. Li and D. S. Lee, *Macromol. Res.,* 2017, **25(6)**, 480.
4. H. Namazi, R. Rakhshaei, H. Hamishehkar and H. Samadi Kafil, *Int. J. Biol. Macromol.*, 2016, **85**, 327.
5. S. A. Park, S H. Lee and W. D. Kim, *Macromol. Res.,* 2011, **19(7)**, 694.
6. S. Van Vlierberghe, P. Dubruel and E. Schacht, *Biomacromolecules.,* 2011, **12**, 1387.
7. T. R. Hoare and D. S. Kohane, *Polym.,* 2008, **49**, 1993.
8. M. Yadollahi and H. Namazi, *J. Nanopart. Res.,* 2013, **15**, 1563.
9. F. Wahid, J. J. Yin, D. D. Xue, H. Xue, Y. S. Lu, C. Zhong and L. Q. Chu, *Int. J. Biol. Macromol.,* 2016, **88**, 273.
10. X. Bai, Z. Bao, S. Bi, Y. Li, X. Yu, S. Hu, M. Tian, X. Zhang, X. Cheng and X. Chen, *Macromol. Biosci.,* 2018, **18**, 3.
11. D. Archana, B. K. Singh, J. Dutta and P. K. Dutta, *Int. J. Biol. Macromol.,* 2015, **73**, 49.
12. D. Archana, B. K. Singh, J. Dutta and P. K. Dutta, *Carbohyd. Polym.,* 2013, **95**, 530.
13. S. Khan, N. Akhtar, M. U. Minhas and S. F. Badshah, *AAPS PharmSciTech.,* 2019, **20**, 119.
14. R. R. Mohamed and M. W. Sabaa, *Int. J. Biol. Macromol.,* 2014, **69**, 95.
15. L. Upadhyaya, J. Singh, V. Agarwal, A. C. Pandey, S. P. Verma, P. Das and R. P. Tewari, *Process. Biochem.,* 2015, **50**, 678.
16. F. Wahid, H. S. Wang, Y. S. Lu, C. Zhong and L. Q. Chu, *Int. J. Biol. Macromol.,* 2017, **101**, 690.
17. L. Upadhyaya, J. Singh, V. Agarwal and R. P. Tewari, *Carbohyd. Polym.,* 2013, **91**, 452.
18. L. Upadhyaya, J. Singh, V. Agarwal and R. P. Tewari, *J. Control. Release*, 2014, **186**, 54.
19. C. Riedo, F. Caldera, T. Poli and O. Chiantore, *Harit. Sci.,* 2015, **3**, 33.
20. N. M. Ranjha and S. Khan, *J. Pharm. Altern. Med.,* 2013, **2**, 30.
21. L. Zhao, H. Mitomo, M. Zhai, F. Yoshii, N. Nagasawa and T. Kume, *Carbohyd. Polym.,* 2003, **53**, 439.
22. Y. Ahmadian, A. Bakravi, H. Hashemi and H. Namazi, *Polym. Bull.,* 2018, **76**, 1967.
23. M. W. Sabaa, H. M. Abdallah, N. A. Mohamed and R. R. Mohamed, *Mat. Sci. Eng. C,* 2015, **56**, 363.
24. S. Agnihotri, S. Mukherji and S. Mukherji, *Appl. Nanosci.,* 2012, **2**, 179.
25. M. Malmsten, *Soft Matter,* 2011, **7**, 8725.
26. V. K. Sharma, R. A. Yngard and Y. Lin, *Adv. Colloid. Interfac.,* 2009, **145(1)**, 83.
27. K. A. Juby, C. Dwivedi, M. Kumar, S. Kota, H. S. Misra and P. N. Bajaj, *Carbohyd. Polym.,* 2012, **89**, 906.
28. P. R. Reddy, K. Varaprasad, R. Sadiku, K. Ramam, G. V. S. Reddy, K. M. Raju and N. S. Reddy, *J. Inorg. Organomet. P,* 2013, **23**, 1054.
29. K. Varaprasad, Y. M. Mohan, K. Vimala and K. Mohana Raju, *J. App. Polym. Sci.,* 2011, **121**, 784.

30. A. Hebeish, M. Hashem, M. M. Abd El-Hady and S. Sharaf, *Carbohyd. Polym.,* 2013, **92**, 407.
31. M. T. Khorasani, A. Joorabloo, A. Moghaddam, H. Shamsi and Z. Mansoori Moghadam, *Int. J. Biol. Macromol.,* 2018, **114**, 1203.
32. F. Song, X. Li, Q. Wang, L. Liao and C. Zhang, *J. Biomed. Nanotechnol.,* 2015, **11**, 40.
33. I. Gholamali, M. Asnaashariisfahani and E. Alipour, *Regen. Eng. Transl. Med.,* 2019, 1.
34. M. Rasoulzadeh and H. Namazi, *Carbohyd. Polym.,* 2017, **168**, 320.
35. Z. Mohamadnia, M. J. Zohuriaan-Mehr, K. Kabiri and M. Razavi-Nouri, *J. Polym. Res.,* 2008, **15**, 173.
36. M. Yadollahi, I. Gholamali, H. Namazi and M. Aghazadeh, *Int. J. Biol. Macromol.,* 2015, **74**, 136.
37. S. Barkhordari, M. Yadollahi and H. Namazi, *J. Polym. Res.,* 2014, **21(6)**, 1.
38. Z. Zare-Akbari, H. Farhadnejad, B. Furughi-Nia, S. Abedin, M. Yadollahi and M. Khorsand-Ghayeni, *Int. J. Biol. Macromol.,* 2016, **93**, 1317.
39. M. Rasoulzadehzali and H. Namazi, *Int. J. Biol. Macromol.,* 2018, **116**, 54.
40. A. P. Ingle, N. Duran and M. Rai, *Appl. Microbial. Bio.,* 2013, 1.
41. D. Das, B. C. Nath, P. Phukon and S. K. Dolui, *Colloid Surface B,* 2013, **101**, 430.
42. K. Gopalakrishnan, C. Ramesh, V. Ragunathan and M. Thamilselvan, *Dig. J. Nanomater. Bio.,* 2012, **7(2)**, 833.
43. S. Zakhireh, M. Mahkam, M. Yadollahi and S. Jafarirad*, J. Polym. Res.,* 2014, **21**, 1.
44. A. Pourjavadi, H. Ghasemzadeh and R. Soleyman, *J. Appl. Polym Sci*., 2007, **105**, 2631.
45. Z. Shariatinia, *Int. J. Biol. Macromol.,* 2018, **120**, 1406.
46. P. S. Gils, D. Ray and P. K. Sahoo, *Int. J. Biol. Macromol.,* 2010, **46**, 237.
47. K. Vimala, K. Samba Sivudu, Y. Murali Mohan, B. Sreedhar and K. Mohana Raju, *Carbohyd. Polym.,* 2009, **75**, 463.
48. Y. Xiang and D. Chen, *Eur. Polym. J.,* 2007, **43**, 4178.
49. T. Jayaramudu, G. M. Raghavendra, K. Varaprasad, R. Sadiku, K. Ramam and K. M. Raju, *Carbohyd. Polym.,* 2013, **95**, 188.
50. T. Jayaramudu, G. M. Raghavendra, K. Varaprasad, R. Sadiku and K. M. Raju, *Carbohyd. Polym.,* 2013, **92**, 2193.
51. M. Yadollahi, I. Gholamali, H. Namazi and M. Aghazadeh, *Int. J. Biol. Macromol.,* 2015, **73**, 109.